THE JOURNAL OF PHYSICAL CHEMISTRY B

A JOURNAL OF THE AMERICAN CHEMICAL SOCIETY

September 8, 2022
Volume 126
Number 35
pubs.acs.org/JPCB

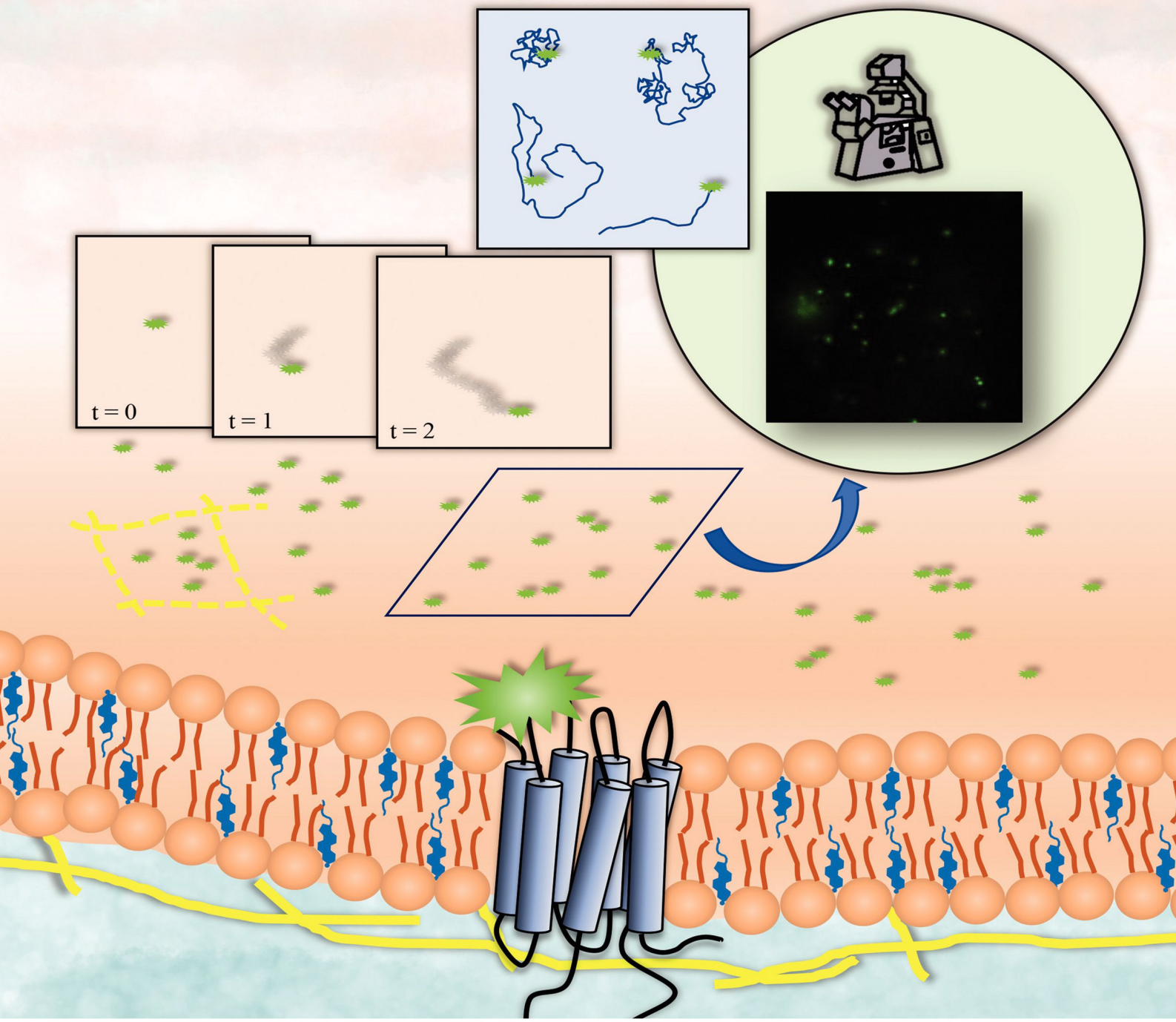

ACS Publications
Most Trusted. Most Cited. Most Read.

www.acs.org

THE JOURNAL OF PHYSICAL CHEMISTRY B
A JOURNAL OF THE AMERICAN CHEMICAL SOCIETY

pubs.acs.org/JPCB

Article

Cholesterol-Dependent Dynamics of the Serotonin$_{1A}$ Receptor Utilizing Single Particle Tracking: Analysis of Diffusion Modes

Published as part of The Journal of Physical Chemistry virtual special issue "Steven G. Boxer Festschrift".

Sandeep Shrivastava, Parijat Sarkar, Pascal Preira, Laurence Salomé, and Amitabha Chattopadhyay*

Cite This: *J. Phys. Chem. B* 2022, 126, 6682−6690

Read Online

ACCESS | Metrics & More | Article Recommendations | Supporting Information

ABSTRACT: G protein-coupled receptors (GPCRs) are signaling hubs in cell membranes that regulate a wide range of physiological processes and are popular drug targets. Serotonin$_{1A}$ receptors are important members of the GPCR family and are implicated in neuropsychiatric disorders. Cholesterol is a key constituent of higher eukaryotic membranes and is believed to contribute to the segregated distribution of membrane constituents into domains. To explore the role of cholesterol in lateral dynamics of GPCRs, we utilized single particle tracking (SPT) to monitor diffusion of serotonin$_{1A}$ receptors under acute and chronic cholesterol-depleted conditions. Our results show that the short-term diffusion coefficient of the receptor decreases upon cholesterol depletion, irrespective of the method of cholesterol depletion. Analysis of SPT trajectories revealed that relative populations of receptors undergoing various modes of diffusion change upon cholesterol depletion. Notably, in cholesterol-depleted cells, we observed an increase in the confined population of the receptor accompanied by a reduction in diffusion coefficient for chronic cholesterol depletion. These results are supported by our recent work and present observations that show polymerization of G-actin in response to chronic cholesterol depletion. Taken together, our results bring out the interdependence of cholesterol and actin cytoskeleton in regulating diffusion of GPCRs in membranes.

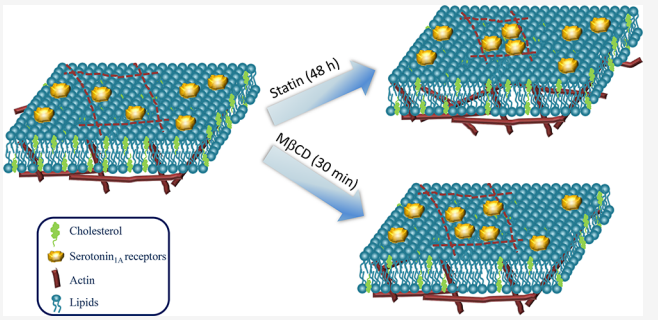

INTRODUCTION

Plasma membranes are complex, quasi-two-dimensional, noncovalent, organized assemblies of various lipids and proteins that allow confinement of cellular contents and offer an appropriate environment to maintain normal functioning of membrane proteins.[1] Besides acting as an interface between the extracellular and intracellular space, biomembranes facilitate communication between cellular exterior and interior via signal transduction. Our current understanding of biological membranes has progressed significantly starting from the "fluid mosaic model" proposed by Singer and Nicolson[2] to a dynamic and complex macromolecular heterogeneous assembly of lipids and proteins often distributed nonrandomly in the membrane.[3,4] In addition, cell membranes are often crowded,[5] and the organization of membrane constituents in this nonhomogeneous milieu involves the concept of lateral heterogeneities, collectively called "membrane domains".[6−9] These specialized domains are thought to be enriched in specific membrane proteins and lipids (such as cholesterol and sphingolipids) which are further held together by the actin cytoskeleton underlying the membrane. These specialized areas on the membrane act as portals for processes such as vesicle trafficking, protein sorting, signal transduction, and entry of pathogens, which span a wide range of spatiotemporal scale.[10−13] Because membrane proteins are embedded in lipids, knowledge of the role of membrane lipids in regulating the dynamics of membrane proteins would help in a better understanding of membrane function.

Cholesterol is an essential lipid in higher eukaryotic cellular membranes and is crucial in the maintenance of membrane structure, dynamics, and function.[14−16] Cholesterol is often nonrandomly distributed in specialized domains in biological and model membranes.[6,17−19] Some of these domains (sometimes referred as "lipid rafts") have been proposed to play an important role in the organization and function of plasma membranes. The concept of such specialized domains on the membrane assumes relevance in the physiology of cells because crucial membrane functions such as signal transduction processes,[20] sorting and trafficking,[21] and the entry of pathogens[13,22,23] have been associated with these regions.

Received: June 7, 2022
Revised: August 1, 2022
Published: August 16, 2022

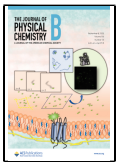

Cholesterol is the end product of a long, multistep, and highly regulated enzymatic pathway orchestrated by more than 20 different enzymes.[24] Notably, cholesterol lowering agents such as statins (one of the top-selling drugs in clinical history) competitively inhibit the enzyme HMG-CoA reductase which acts in the rate-limiting step of cholesterol biosynthesis.[25−28] Recent evidence has suggested that the modulation of membrane cholesterol using statins could alter the polymerization status of the actin cytoskeleton, thereby constituting an evolving feature associated with the regulation of membrane composition and organization.[29−32] Importantly, both cholesterol and the actin cytoskeleton have been shown to alter the lateral dynamics of membrane proteins such as G protein-coupled receptors (GPCRs)[33−35] which serve as major drug targets across all clinical areas.[36−38]

GPCRs are the largest and most diverse class of proteins in higher eukaryotic plasma membranes that regulate a wide array of signaling processes across the membrane.[36,39,40] They play an important role in a large number of physiological processes such as neurotransmission, cellular metabolism, cellular differentiation, and immune response. As a result of their involvement in crucial biological processes, GPCRs have emerged as major therapeutic targets[37,41] and account for ∼40% of currently approved drugs.[38] The serotonin$_{1A}$ receptor, an important neurotransmitter receptor which belongs to the GPCR family, is extensively studied among the serotonin receptors and mediates a gamut of neurological, cognitive, and behavioral functions.[42−48] Because the serotonin$_{1A}$ receptor plays an essential role in human physiology, it represents a major therapeutic target in developing drugs against neuropsychiatric disorders such as depression, anxiety, and even cancer.[49,50]

Lateral diffusion of membrane proteins represents a fundamental physical property that regulates the dynamics of protein−protein and lipid−protein interactions, which in turn regulates their function.[51,52] Membrane proteins often undergo confined lateral diffusion, which arises due to compositional heterogeneity in cell membranes and the actin cytoskeleton, that could span different spatiotemporal scales.[53] The presence of an intricate network of actin cytoskeleton below the membrane constitutes a major source of confined lateral diffusion in membranes.[29,54,55] Several observations using high-resolution microscopy based approaches have recognized the role of the actin cytoskeleton as a key factor that determines the dynamics of membrane proteins.[35,56−58] Measurement of membrane dynamics is often challenging due to the inherent noise in cellular systems. A variety of microscopy-based techniques have been established to measure diffusion in heterogeneous biological membranes. The widely used approaches to probe lateral dynamics in membranes are fluorescence recovery after photobleaching (FRAP), fluorescence correlation spectroscopy (FCS), and single particle tracking (SPT).[52,59−62] In recent years, significant progress has been made toward the measurement and interpretation of membrane dynamics at the single-molecule level that helps detection and tracking of individual membrane-bound molecules under physiological conditions with a high spatiotemporal resolution.[63−66] The advantage of single-molecule measurement is that it allows to circumvent ensemble averaging from multiple molecules, thereby providing information about the heterogeneous behavior (and transient phenomena) within subpopulations of molecules.[67]

SPT has emerged as a powerful approach to monitor lateral diffusion and organization of membrane lipids and proteins.[55,60,61,66,68,69] Although single particle tracking has been utilized to measure dynamics of membrane proteins,[63,70] the application of SPT to GPCRs is relatively limited.[58,64,71,72] In this work, we explored the diffusion characteristics of the human serotonin$_{1A}$ receptor in live cells under acute and chronic cholesterol depleted conditions utilizing SPT. Analysis of GPCR diffusion in the membrane helps understand GPCR function and provides insight into cellular signaling.[52] By analysis of diffusion modes, we show how acute and chronic cholesterol depletion could influence diffusion behavior of the serotonin$_{1A}$ receptor, which could have crucial implications in GPCR function.

METHODS

Materials. BSA, $CaCl_2$, methyl-β-cyclodextrin (MβCD), DMSO, doxycycline, D-glucose, EDTA, gentamycin sulfate, $MgCl_2$, $MnCl_2$, $NaHCO_3$, penicillin, poly(L-lysine), streptomycin, Triton X-100, and Tris were purchased from Sigma (St. Louis, MO). Qdot 655 streptavidin conjugate, Alexa Fluor 546 phalloidin, and Amplex Red cholesterol assay kit were obtained from Molecular Probes/Invitrogen (Eugene, OR). Antimyc tag antibody C-terminal (Biotin) was obtained from Abcam (Cambridge, UK). Antimyc antibody Alexa Fluor 488 conjugate was purchased from Millipore (Bedford, MA). Lovastatin was purchased from Calbiochem (San Diego, CA). DMEM/F-12 (Dulbecco's modified Eagle medium: nutrient mixture F-12 (Ham) (1:1)), hygromycin, and fetal calf serum were obtained from Invitrogen/Life Technologies (Grand Island, NY). Water was purified through a Millipore (Bedford, MA) Milli-Q system and used throughout.

Cell Culture and Treatment. HEK-293 cells stably expressing the N-terminal myc-tagged serotonin$_{1A}$ receptor (HEK-5-HT$_{1A}$R) were generated as described previously.[73] The stock solution of lovastatin was prepared as described previously.[74] Cells grown for 24 h were incubated with 2.5 μM lovastatin in complete DMEM/F-12 medium for 48 h in a humidified atmosphere at 37 °C with 5% CO_2. Control cells were grown without lovastatin under similar conditions. Acute cholesterol depletion was performed using MβCD as described previously.[75] Briefly, after growing cells for 3 days in complete DMEM/F-12 medium, cells were incubated in serum-free DMEM/F-12 medium for 3 h in a humidified atmosphere at 37 °C with 5% CO_2. Cholesterol depletion was performed by treating cells with 5 mM MβCD in serum-free DMEM/F-12 medium for 30 min in a humidified atmosphere at 37 °C with 5% CO_2, followed by washing with PBS. See the Supporting Information (Section S1) for more details.

Receptor Localization Using Confocal Microscopic Imaging. HEK-5-HT$_{1A}$R cells were seeded at a density of ∼10^4 cells on 22 × 22 mm glass coverslips and grown for 3 days as described earlier.[58] Serotonin$_{1A}$ receptors were labeled with the antimyc antibody Alexa Fluor 488 conjugate and imaged by an inverted Zeiss LSM 880 confocal microscope (Jena, Germany) with a 488 nm argon laser, and emission was collected from 500 to 560 nm. See the Supporting Information (Section S2) for more details.

Estimation of Cellular Cholesterol Content. An Amplex Red cholesterol assay kit was used to estimate cholesterol content from cell lysates obtained from control, 2.5 μM lovastatin-treated, and 5 mM MβCD-treated cells.[76] Choles-

https://doi.org/10.1021/acs.jpcb.2c03941
J. Phys. Chem. B 2022, 126, 6682−6690

terol content values were normalized to total cellular protein estimated by using the BCA assay.[77]

Single Particle Tracking Experiments. Serotonin$_{1A}$ receptors in HEK-5-HT$_{1A}$R cells were labeled with antibody conjugated quantum dots (QDs) for SPT measurements. A Cascade II 512 EM-CCD camera (Roper Scientific, Tucson, AZ) operating at 25 Hz acquisition frequency on a Zeiss Axio-observer A1 microscope (Jena, Germany) at room temperature (~22 °C) was used to track the trajectories of QDs at the cell surface. The Multiple Target Tracing program developed by Sergé et al.[78] was used to analyze the trajectories of all QDs in a video sequence. The diffusion coefficient inside the confined trajectory segments and the size of the domains (or radius of confinement (R)) were determined by fitting MSD(t) with its theoretical expression for confined diffusion.[79] See the Supporting Information (Section S3) for more details.

F-Actin Labeling of Cells. F-actin labeling in HEK-5-HT$_{1A}$R cells under control (without treatment), 2.5 μM lovastatin-treated, and 5 mM MβCD-treated conditions was performed by using Alexa Fluor 546 phalloidin as described previously.[32,80,81] See the Supporting Information (Section S4) for more details.

Quantitation of F-Actin. F-actin was imaged by using an inverted Zeiss LSM 510 Meta confocal microscope (Jena, Germany). F-actin quantitation in HEK-5-HT$_{1A}$R cells under control (without treatment), 2.5 μM lovastatin-treated, and 5 mM MβCD-treated conditions was performed as described previously.[32,80,81] See the Supporting Information (Section S5) for more details.

RESULTS AND DISCUSSION

In this work, we utilized HEK-293 cells stably expressing the N-terminal myc-tagged serotonin$_{1A}$ receptor (HEK-5-HT$_{1A}$R, see Figure 1a) to explore the role of cholesterol on receptor dynamics (lateral diffusion). The serotonin$_{1A}$ receptor expressed in HEK-5-HT$_{1A}$R cells is predominantly localized on the plasma membrane as shown in a representative confocal microscopic image at a midplane section of a cell (see Figure 1b). Notably, we previously demonstrated that serotonin$_{1A}$ receptors heterologously expressed in HEK-5-HT$_{1A}$R cells could mimic the pharmacological and cellular function of the native receptors in terms of ligand binding, coupling to G proteins, cAMP signaling, and cellular trafficking.[73,82] In addition, the N-terminal myc-tag allows tracking the trajectory of the serotonin$_{1A}$ receptor using SPT by fluorescently labeling the receptor in HEK-5-HT$_{1A}$R cells with quantum dots (QD) conjugated to streptavidin which are precoupled to a biotinylated anti-c-myc antibody.

Signal transduction mediated by membrane-bound receptors has been proposed to involve differential lateral mobility of various interacting partners in the membrane.[83−85] This constitutes the basis of the "mobile receptor" hypothesis which proposes that lateral diffusion determines the interaction between receptor and effector molecules and subsequent signaling at the plasma membrane.[52] Because signaling via GPCRs involves the functional interaction of effector molecules in a heterogeneous membrane environment, the spatiotemporal dynamics of these components in membranes acts as a determining factor of the signaling output by these receptors.[35,52] To explore the role of membrane cholesterol in regulating the diffusion of the serotonin$_{1A}$ receptor, we depleted cholesterol from HEK-5-HT$_{1A}$R cells using both chronic and acute cholesterol depletion methods. The main

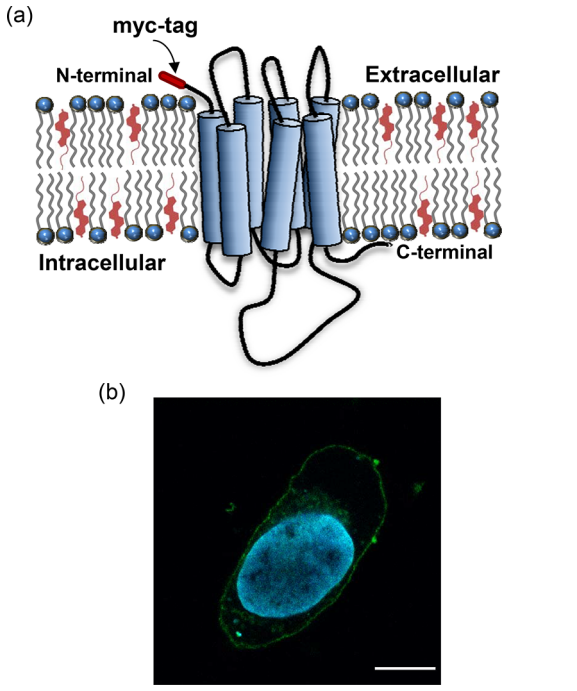

Figure 1. Features of the human serotonin$_{1A}$ receptor in HEK-293 cells. (a) A schematic representation of the topological features of the serotonin$_{1A}$ receptor with a myc-tag (maroon) at its N-terminal. The membrane is shown as a bilayer of phospholipids (headgroup shown in blue) containing cholesterol (shown in red). (b) A representative confocal microscopic midplane section image of the serotonin$_{1A}$ receptor stably expressed in HEK-293 cells (HEK-5-HT$_{1A}$R cells). Serotonin$_{1A}$ receptors were labeled with antimyc antibody conjugated to Alexa Fluor 488 (green), and the nucleus was labeled with DAPI (blue). The scale bar represents 10 μm.

difference between chronic and acute cholesterol depletion methods is the experimental time scale associated with the two processes.[32,86] Acute cholesterol depletion involves physical removal of cholesterol using carriers such as MβCD, a water-soluble carbohydrate polymer with a central nonpolar cavity, that efficiently and selectively extracts membrane cholesterol in a relatively short time (approximately minutes).[87,88] On the other hand, chronic cholesterol depletion is performed over a longer time period (approximately days) by using cholesterol biosynthetic inhibitors that mimic physiological conditions.[89] Cholesterol lowering agents such as statins are extensively used for chronic cholesterol depletion and represent some of the best-selling oral cholesterol-lowering drugs.[26,27] Statins competitively inhibit the rate-limiting enzyme HMG-CoA reductase in the cellular cholesterol biosynthetic pathway.[25] Figure 2 shows the cholesterol content in cell lysates from cholesterol-depleted HEK-5-HT$_{1A}$R cells. The cellular cholesterol content exhibited reduction upon treatment with lovastatin and MβCD. For example, cholesterol content was reduced to ~40% of control (without treatment) in lysates from HEK-5-HT$_{1A}$R cells treated with 5 mM MβCD. HEK-5-HT$_{1A}$R cells treated with 2.5 μM lovastatin show ~7% reduction in cholesterol content relative to control cell lysates.

To ensure the reliability of the single-particle tracking measurements, we optimized the experimental conditions before acquiring the systematic video sequences. We first tested the specificity of QDs for labeling the N-terminally myc-tagged serotonin$_{1A}$ receptor. We observed fluorescence signal from ~20 QDs per cell when HEK-5-HT$_{1A}$R cells were

https://doi.org/10.1021/acs.jpcb.2c03941
J. Phys. Chem. B 2022, 126, 6682−6690

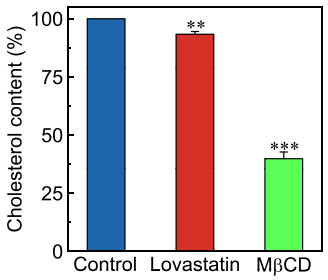

Figure 2. Cholesterol content of lysates from HEK-5-HT$_{1A}$R cells. Cholesterol content was estimated in lysates from HEK-5-HT$_{1A}$R cells treated with 2.5 μM lovastatin or 5 mM MβCD (** and *** correspond to significant ($p < 0.01$ and $p < 0.001$) difference in cholesterol content in lovastatin- and MβCD-treated cells, respectively, relative to control cells). Values are normalized to cholesterol content in control (untreated) cells. Data represent means ± SE of three independent experiments.

incubated with streptavidin-conjugated QDs precoupled to biotinylated anti-c-myc antibody. These QDs remained bound even after washing the cells several times. In contrast, we found only 2−3 QDs on each cell in the case of labeling with QDs alone (without prior coupling to biotinylated anti-c-myc antibody). We recorded a series of 80 s video sequences for each cell with varied antibody/QD ratios to calculate the short-term diffusion coefficient (D_{1-2}, where "1−2" refers to the first two points of the MSD. In accordance with previous literature,[90] we chose the antibody/QD ratio of 1:10 for our SPT experiments to minimally perturb receptor diffusion (more detailed examination of labeling artifacts requires further investigation). We could obtain analyzable tracks from those QDs that were present on top of the cells. Data acquisition was performed in control (without treatment), 2.5 μM lovastatin-treated, and 5 mM MβCD-treated HEK-5-HT$_{1A}$R cells using these conditions. As a first step, we performed a global analysis of all trajectories collected for each condition. Figure 3 shows the distributions of the short-term diffusion coefficient D_{1-2} for control and cholesterol-depleted conditions. As shown in the figure, we observed a shift in the distribution of D_{1-2} toward lower values for lovastatin- and MβCD-treated cells relative to the control condition. The average D_{1-2} value for control cells was $(4.4 \pm 0.3) \times 10^{-2}$ μm^2 s^{-1} (data represent means ± SE). The short-term diffusion coefficient of the serotonin$_{1A}$ receptor obtained by using the SPT method was found to be similar to the diffusion coefficient obtained for other class A GPCRs such as the neurokinin-1 receptor[72] and the μ-opioid receptor.[71] The values of average D_{1-2} for cells treated with lovastatin and MβCD were found to be $(3.0 \pm 0.3) \times 10^{-2}$ and $(2.5 \pm 0.2) \times 10^{-2}$ μm^2 s^{-1}, respectively. Such a reduction in diffusion coefficient of membrane proteins upon cholesterol depletion has been reported earlier[72,74,91−93] and could be due to the further compartmentalization of the plasma membrane driven by enhanced actin polymerization under these conditions.[32] In addition, the reduction observed in diffusion coefficient upon acute cholesterol depletion could be due to the inherent regional microheterogeneity in the plasma membrane.[92,94]

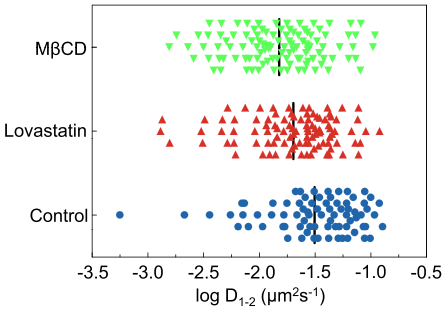

Figure 3. Distribution of diffusion coefficient of serotonin$_{1A}$ receptors determined by SPT. Distribution of short-term diffusion coefficient (log D_{1-2}) calculated from the trajectories of serotonin$_{1A}$ receptors obtained by SPT in control (blue circles, $n = 77$), 2.5 μM lovastatin-treated (red triangles, $n = 101$), and 5 mM MβCD-treated (inverted green triangles, $n = 102$) HEK-5-HT$_{1A}$R cells. The time duration for the video recordings was set to 80 s, and other details are as described previously.[58]

SPT provides specific information about lateral dynamics of single particles in a well-resolved spatiotemporal scale which is crucial for the study of complex biological membranes. A characteristic feature of SPT measurements is that it allows diffusion analysis of individual trajectories and therefore the distribution of these trajectories among different diffusion modes could be analyzed. In addition, SPT allows to distinguish subpopulations of molecules undergoing different modes of diffusion, which is very useful to understand the microheterogeneity (domains) in membranes. We identified four diffusion modes by analysis of video trajectories: random, confined, transiently confined, and directed diffusion (Figure 4). Interestingly, upon acute cholesterol depletion (using MβCD), the fraction of trajectories characterized by random diffusion mode exhibited reduction. In addition, both chronic and acute cholesterol depletion led to an increase in confined diffusion mode relative to control condition (see Figure 4a). Along with the change in various diffusion modes, we observed significant changes in the diffusion coefficient (D_{1-2}) of the serotonin$_{1A}$ receptor among different diffusion modes. For example, we observed a significant decrease in D_{1-2} for random diffusion mode upon statin treatment (see Figure 4b). On the other hand, D_{1-2} for confined population remain invariant, whereas D_{1-2} for transiently confined mode exhibited a significant reduction upon acute and chronic cholesterol depletion (Figure 4b). These observations are supported by previous reports suggesting that cholesterol depletion results in the rearrangement of the actin cytoskeleton.[92,31,32] The generation of these compartments (domains) on the cell membrane could be attributed to the polymerization of the actin cytoskeleton which induces dynamic constraints on receptor diffusion and therefore reduces the population of random diffusion along with a concomitant increase in confined (or transiently confined) diffusion modes.

The effect of the increase in dynamic constraints upon chronic cholesterol depletion gets further manifested in the serotonin$_{1A}$ receptor diffusion, as evident from the overall reduction in the distribution of the radius of confinement (R) and an overall shift toward lower values of the confinement radius (see Table 1 and Figure 5). The average radius of confinement was ∼213 nm for receptors undergoing confined diffusion in control cells (Table 1). The corresponding values for the average radius of confinement upon chronic cholesterol depletion showed a prominent reduction. The average radius of confinement undergoing confined diffusion values for receptors under chronic cholesterol depleted condition was ∼176 nm, resulting in ∼17% reduction relative to the control condition (Table 1). The average radius of confinement upon

https://doi.org/10.1021/acs.jpcb.2c03941
J. Phys. Chem. B 2022, 126, 6682−6690

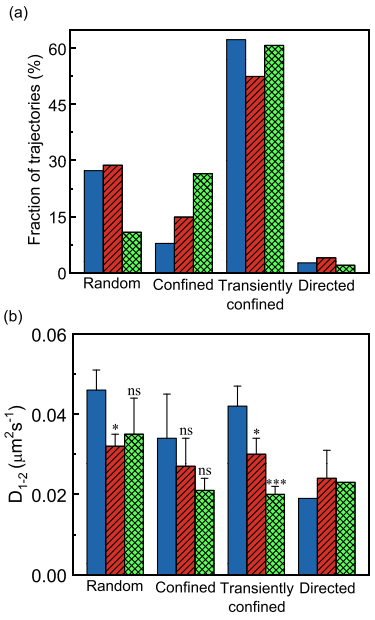

Figure 4. (a) Relative distribution of SPT trajectories of serotonin$_{1A}$ receptors among the four diffusion modes. The relative distribution of SPT trajectories of serotonin$_{1A}$ receptors in HEK-5-HT$_{1A}$R cells among the four diffusion modes observed in control (blue bars, n = 77), 2.5 μM lovastatin-treated (red hatched bars, n = 101), and 5 mM MβCD-treated (green criss-crossed bars, n = 102) conditions. (b) Average short-term diffusion coefficient (D_{1-2} (μm^2 s^{-1})) of the serotonin$_{1A}$ receptor measured by SPT in HEK-5-HT$_{1A}$R cells for each diffusion mode in control (blue bars), 2.5 μM lovastatin-treated (red hatched bars), and 5 mM MβCD-treated (green criss-crossed bars) conditions. Data represent means ± SE of at least four independent experiments with at least eight cells for each experiment (* and *** correspond to significant (p < 0.05 and p < 0.001) difference in D_{1-2} for cells treated with 2.5 μM lovastatin and 5 mM MβCD, respectively, relative to control condition). The lack of significance of D_{1-2} values between control and cholesterol-depleted conditions is denoted by ns. See the Methods section and Table 1 for other details.

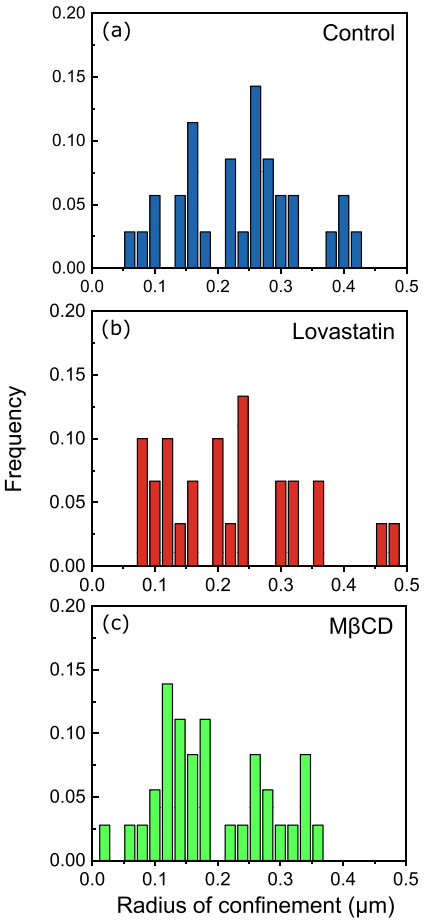

Figure 5. Distribution of domain radii of confinement zones. Histograms for distribution of domain radii of confinement in the confined trajectories measured by SPT for serotonin$_{1A}$ receptors in (a) control (blue bars, n = 48), (b) 2.5 μM lovastatin-treated (red bars, n = 53), and (c) 5 mM MβCD-treated (green bars, n = 62). All other details are as described previously.[58] See the Methods section for other details.

acute cholesterol depletion using MβCD displayed no significant decrease (for the confined population). Overall, these results suggest that dynamic constraints on receptor diffusion upon chronic cholesterol depletion increase, which could lead to the formation of small-sized confined zones induced by the actin cytoskeleton. Interestingly, the transiently confined population showed a significant reduction in radius of

Table 1. Diffusion Parameters of the Serotonin$_{1A}$ Receptor for Different Diffusion Modes

	diffusion modes				
				transiently confined	
	random	confined	directed	random	confined
(a) control					
D_{1-2} (10^{-2} $\mu m^2/s$)	4.6 ± 0.5	3.4 ± 1.1	1.9	5.0 ± 1.6	4.2 ± 0.5
no. of trajectories	21	6	2	48	
R (nm)		213 ± 8			287 ± 30
(b) lovastatin-treated[a]					
D_{1-2} (10^{-2} $\mu m^2/s$)	3.2 ± 0.3	2.7 ± 0.7	2.4 ± 0.7	3.2 ± 0.5	2.9 ± 0.4
no. of trajectories	29	15	4	53	
R (nm)		176 ± 27			263 ± 31
(c) MβCD-treated[b]					
D_{1-2} (10^{-2} $\mu m^2/s$)	3.5 ± 0.9	2.1 ± 0.3	2.3	2.2 ± 0.4	1.9 ± 0.2
no. of trajectories	11	27	2	62	
R (nm)		203 ± 26			214 ± 22

[a]The concentration of lovastatin was 2.5 μM. [b]The concentration of MβCD was 5 mM.

https://doi.org/10.1021/acs.jpcb.2c03941
J. Phys. Chem. B 2022, 126, 6682−6690

confinement upon acute cholesterol depletion (Table 1). This reinforces our previous observations using beam-radius-dependent FRAP that acute cholesterol depletion induces dynamic (transient) confinement of the receptor.[75]

To test whether the observed confinement upon cholesterol depletion was due to change in actin polymerization, we performed quantification of F-actin under acute and chronic cholesterol depleted conditions using a quantitative high-resolution confocal microscopy based approach previously developed by us that allows measurement of F-actin content using an image reconstruction method.[81] To quantitatively estimate the extent of F-actin reorganization, we labeled F-actin with Alexa Fluor 546 conjugated phalloidin (a specific fluorescent probe for F-actin[95]). Figure 6a–c shows

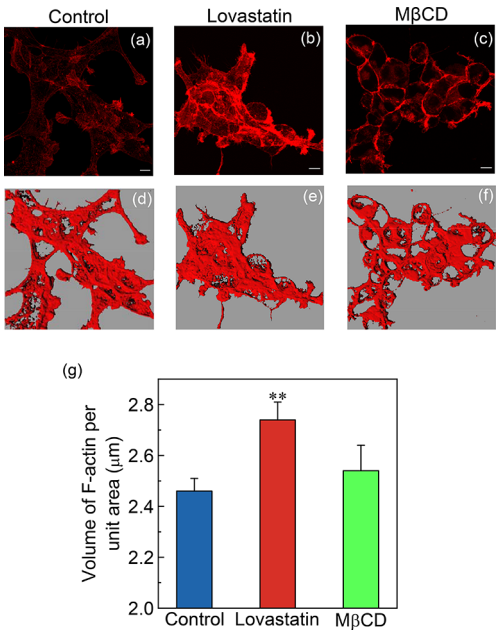

Figure 6. Reorganization of actin cytoskeleton in HEK-5-HT$_{1A}$R cells upon cholesterol depletion. The actin cytoskeleton of HEK-293 cells was labeled with Alexa Fluor 546 phalloidin. The F-actin content was estimated by using a quantitative high-resolution confocal microscopic technique previously developed by us.[81] (a–c) Maximum intensity projections obtained from confocal z sections under control, 2.5 μM lovastatin-treated, and 5 mM MβCD-treated conditions, respectively. The respective isosurfaces corresponding to the z sections are shown in (d–f). The F-actin content values in control, lovastatin-treated, and MβCD-treated cells are shown in (g). Data represent means ± SE of at least 11 independent measurements from three independent experiments (** corresponds to significant (p < 0.01) difference in F-actin content in cells treated with 2.5 μM lovastatin relative to control cells). See the Methods section for other details.

representative confocal micrographs with maximum intensity projections (MIPs) of the actin cytoskeleton under various treatment conditions. The panels in Figure 6d–f represent isosurface maps (contours obtained by joining voxels of equal fluorescence intensity across all z sections) of cellular F-actin corresponding to the projected images shown in Figure 6a–c. To quantitatively estimate cellular F-actin content, we normalized the fluorescence volume enclosed by the isosurface in each case to the projected area of cells. This ratio (fluorescence volume/area of cells) is a measure of the F-actin content in cells and is shown in Figure 6g. As shown in the figure, HEK-5-HT$_{1A}$R cells treated with lovastatin resulted in ∼11% increase in cellular F-actin levels, while MβCD treatment show negligible change in F-actin levels. These results are in overall agreement with our recent observations in CHO-K1 cells where we showed that F-actin content significantly increases upon chronic cholesterol depletion but not in acute cholesterol depletion.[32] In this overall backdrop, the effect of the crosstalk between cholesterol and actin cytoskeleton by quantitatively measuring changes in F-actin content as a consequence of acute and chronic cholesterol depletion on the dynamics of the serotonin$_{1A}$ receptor assumes relevance.

CONCLUSION

We utilized SPT to measure diffusion behavior of the serotonin$_{1A}$ receptor under cholesterol-depleted conditions. The advantage of SPT measurement is its ability to distinguish subpopulations of receptors undergoing various modes of diffusion which yields useful information about complex microheterogeneous environments such as biological membranes. Our results show that the overall short-term diffusion coefficient of the serotonin$_{1A}$ receptor exhibits reduction upon both acute and chronic cholesterol depletion (Figure 3). Notably, we observed a significant increase in the confined receptor population under cholesterol-depleted conditions. Such a change in the subpopulations of the serotonin$_{1A}$ receptor undergoing various modes of diffusion upon cholesterol depletion could have implications on receptor function. These results provide one of the first systematic studies of diffusion behavior of the serotonin$_{1A}$ receptor by using two kinetically different methods of depletion of cholesterol and provides information about the subpopulations of the receptor undergoing various modes of diffusion. Interestingly, our results show that the nature of confinement varies depending on the method of cholesterol depletion. This is due to the fact that whereas chronic cholesterol depletion results in permanent confinement involving remodeling of the actin cytoskeleton, acute cholesterol depletion leads to transient confinement. In addition, this work highlights the role of cholesterol and actin cytoskeleton on the dynamics of the serotonin$_{1A}$ receptor which could be helpful in understanding the correlation between dynamics and function of the serotonin$_{1A}$ receptor. We conclude that measurements of receptor dynamics at varying spatiotemporal scales could provide novel insight toward developing a conceptual framework for cellular signaling.

ASSOCIATED CONTENT

Supporting Information

The Supporting Information is available free of charge at https://pubs.acs.org/doi/10.1021/acs.jpcb.2c03941.

Section S1: cell culture and treatment; Section S2: confocal microscopic imaging of receptor localization; Section S3: single particle tracking experiments; Section S4: F-actin labeling of cells; Section S5: fluorescence microscopy and F-actin quantitation (PDF)

AUTHOR INFORMATION

Corresponding Author

Amitabha Chattopadhyay − *CSIR-Centre for Cellular and Molecular Biology, Hyderabad 500 007, India;* orcid.org/

https://doi.org/10.1021/acs.jpcb.2c03941
J. Phys. Chem. B 2022, 126, 6682−6690

0000-0002-2618-2565; Phone: +91-40-2719-2578; Email: amit@ccmb.res.in

Authors

Sandeep Shrivastava − *CSIR-Centre for Cellular and Molecular Biology, Hyderabad 500 007, India*

Parijat Sarkar − *CSIR-Centre for Cellular and Molecular Biology, Hyderabad 500 007, India;* Present Address: Department of Biochemistry, Stanford University, School of Medicine, Stanford, CA 94305

Pascal Preira − *Institut de Pharmacologie et de Biologie Structurale, CNRS, Université de Toulouse (UPS), 31 077 Toulouse, France*

Laurence Salomé − *Institut de Pharmacologie et de Biologie Structurale, CNRS, Université de Toulouse (UPS), 31 077 Toulouse, France;* orcid.org/0000-0001-9667-4154

Complete contact information is available at: https://pubs.acs.org/10.1021/acs.jpcb.2c03941

Author Contributions

S.S. and P.S. contributed equally to this work.

Notes

The authors declare no competing financial interest.

■ ACKNOWLEDGMENTS

This work was supported by Indo-French Centre for the Promotion of Advanced Research (Project 4603-2) to A.C. and L.S. A.C. gratefully acknowledges support from SERB Distinguished Fellowship and CSIR Bhatnagar Fellowship. P.S. was supported as a Senior Project Associate by a CSIR FBR grant (MLP 0146) to A.C. We gratefully acknowledge members of the Chattopadhyay laboratory and Drs. Bhagyashree Rao (Crick Institute) and G. Aditya Kumar (University of Michigan) for their comments and suggestions.

■ REFERENCES

(1) Pal, S.; Chattopadhyay, A. What is so unique about biomembrane organization and dynamics? In *Membrane Organization and Dynamics*; Chattopadhyay, A., Ed.; Springer: Heidelberg, 2017; pp 1−9.

(2) Singer, S. J.; Nicolson, G. L. The fluid mosaic model of the structure of cell membranes. *Science* **1972**, *175*, 720−731.

(3) Goñi, F. M. The basic structure and dynamics of cell membranes: an update of the Singer-Nicolson model. *Biochim. Biophys. Acta* **2014**, *1838*, 1467−1476.

(4) Levental, I.; Levental, K. R.; Heberle, F. A. Lipid rafts: controversies resolved, mysteries remain. *Trends Cell Biol.* **2020**, *30*, 341−353.

(5) Takamori, S.; Holt, M.; Stenius, K.; Lemke, E. A.; Grønborg, M.; Riedel, D.; Urlaub, H.; Schenck, S.; Brügger, B.; Ringler, P.; et al. Molecular anatomy of a trafficking organelle. *Cell* **2006**, *127*, 831−846.

(6) Mukherjee, S.; Maxfield, F. R. Membrane domains. *Annu. Rev. Cell Dev. Biol.* **2004**, *20*, 839−866.

(7) Jacobson, K.; Mouritsen, O.; Anderson, R. Lipid rafts: at a crossroad between cell biology and physics. *Nat. Cell Biol.* **2007**, *9*, 7−14.

(8) Simons, K.; Sampaio, J. L. Membrane organization and lipid rafts. *Cold Spring Harb. Perspect. Biol.* **2011**, *3*, a004697.

(9) Levental, I.; Veatch, S. The continuing mystery of lipid rafts. *J. Mol. Biol.* **2016**, *428*, 4749−4764.

(10) Chichili, G. R.; Rodgers, W. Cytoskeleton-membrane interactions in membrane raft structure. *Cell. Mol. Life Sci.* **2009**, *66*, 2319−2328.

(11) Byrum, J. N.; Rodgers, W. Membrane-cytoskeleton interactions in cholesterol-dependent domain formation. *Essays Biochem.* **2015**, *57*, 177−187.

(12) Sezgin, E.; Levental, I.; Mayor, S.; Eggeling, C. The mystery of membrane organization: composition, regulation and roles of lipid rafts. *Nat. Rev. Mol. Cell Biol.* **2017**, *18*, 361−374.

(13) Kumar, G. A.; Jafurulla, M.; Chattopadhyay, A. The membrane as the gatekeeper of infection: Cholesterol in host-pathogen interaction. *Chem. Phys. Lipids* **2016**, *199*, 179−185.

(14) Simons, K.; Ikonen, E. How cells handle cholesterol. *Science* **2000**, *290*, 1721−1725.

(15) Mouritsen, O. G.; Zuckermann, M. J. What's so special about cholesterol? *Lipids* **2004**, *39*, 1101−1113.

(16) Kumar, G. A.; Chattopadhyay, A. Cholesterol: an evergreen molecule in biology. *Biomed. Spectrosc. Imaging* **2016**, *5*, S55−S66.

(17) Lingwood, D.; Simons, K. Lipid rafts as a membrane-organizing principle. *Science* **2010**, *327*, 46−50.

(18) Chaudhuri, A.; Chattopadhyay, A. Transbilayer organization of membrane cholesterol at low concentrations: implications in health and disease. *Biochim. Biophys. Acta* **2011**, *1808*, 19−25.

(19) Xu, X.; London, E. The effect of sterol structure on membrane lipid domains reveals how cholesterol can induce lipid domain formation. *Biochemistry* **2000**, *39*, 843−849.

(20) Simons, K.; Toomre, D. Lipid rafts and signal transduction. *Nat. Rev. Mol. Cell Biol.* **2000**, *1*, 31−39.

(21) Simons, K.; van Meer, G. Lipid sorting in epithelial cells. *Biochemistry* **1988**, *27*, 6197−6202.

(22) Riethmüller, J.; Riehle, A.; Grassmé, H.; Gulbins, E. Membrane rafts in host-pathogen interactions. *Biochim. Biophys. Acta* **2006**, *1758*, 2139−2147.

(23) Pucadyil, T. J.; Chattopadhyay, A. Cholesterol: A potential therapeutic target in Leishmania infection? *Trends Parasitol.* **2007**, *23*, 49−53.

(24) Nes, W. D. Biosynthesis of cholesterol and other sterols. *Chem. Rev.* **2011**, *111*, 6423−6451.

(25) Istvan, E. S.; Deisenhofer, J. Structural mechanism for statin inhibition of HMG-CoA reductase. *Science* **2001**, *292*, 1160−1164.

(26) Endo, A. A historical perspective on the discovery of statins. *Proc. Japan Acad. Ser. B Phys. Biol. Sci.* **2010**, *86*, 484−493.

(27) Goldstein, J. L.; Brown, M. S. A century of cholesterol and coronaries: From plaques to genes to statins. *Cell* **2015**, *161*, 161−172.

(28) Brown, A. J.; Sharpe, L. J. Cholesterol synthesis. In *Biochemistry of Lipids, Lipoproteins and Membranes*; Ridgway, N. D., McLeod, R. S., Eds.; Elsevier: Amsterdam, 2016; pp 327−358.

(29) Kwik, J.; Boyle, S.; Fooksman, D.; Margolis, L.; Sheetz, M. P.; Edidin, M. Membrane cholesterol, lateral mobility, and the phosphatidylinositol 4,5-bisphosphate-dependent organization of cell actin. *Proc. Natl. Acad. Sci. U. S. A.* **2003**, *100*, 13964−13969.

(30) Tsai, H. I.; Tsai, L. H.; Chen, M. Y.; Chou, Y. C. Cholesterol deficiency perturbs actin signaling and glutamate homeostasis in hippocampal astrocytes. *Brain Res.* **2006**, *1104*, 27−38.

(31) Sun, M.; Northup, N.; Marga, F.; Huber, T.; Byfield, F. J.; Levitan, I.; Forgacs, G. The effect of cellular cholesterol on membrane-cytoskeleton adhesion. *J. Cell Sci.* **2007**, *120*, 2223−2231.

(32) Sarkar, P.; Kumar, G. A.; Shrivastava, S.; Chattopadhyay, A. Chronic cholesterol depletion increases F-actin levels and induces cytoskeletal reorganization via a dual mechanism. *J. Lipid Res.* **2022**, *63*, 100206.

(33) Pucadyil, T. J.; Kalipatnapu, S.; Harikumar, K. G.; Rangaraj, N.; Karnik, S. S.; Chattopadhyay, A. G-protein-dependent cell surface dynamics of the human serotonin$_{1A}$ receptor tagged to yellow fluorescent protein. *Biochemistry* **2004**, *43*, 15852−15862.

(34) Jaqaman, K.; Grinstein, S. Regulation from within: The cytoskeleton in transmembrane signaling. *Trends Cell Biol.* **2012**, *22*, 515−526.

(35) Ganguly, S.; Pucadyil, T. J.; Chattopadhyay, A. Actin cytoskeleton-dependent dynamics of the human serotonin$_{1A}$ receptor correlates with receptor signaling. *Biophys. J.* **2008**, *95*, 451−463.

(36) Chattopadhyay, A. GPCRs: Lipid-dependent membrane receptors that act as drug targets. *Adv. Biol.* **2014**, *2014*, 143023.
(37) Sriram, K.; Insel, P. A. G protein-coupled receptors as targets for approved drugs: how many targets and how many drugs? *Mol. Pharmacol.* **2018**, *93*, 251−258.
(38) Chan, H. C. S.; Li, Y.; Dahoun, T.; Vogel, H.; Yuan, S. New binding sites, new opportunities for GPCR drug discovery. *Trends Biochem. Sci.* **2019**, *44*, 312−330.
(39) Katritch, V.; Cherezov, V.; Stevens, R. C. Structure-function of the G protein-coupled receptor superfamily. *Annu. Rev. Pharmacol. Toxicol.* **2013**, *53*, 531−556.
(40) Sakmar, T. P. Introduction: G-protein coupled receptors. *Chem. Rev.* **2017**, *117*, 1−3.
(41) Jacobson, K. A. New paradigms in GPCR drug discovery. *Biochem. Pharmacol.* **2015**, *98*, 541−555.
(42) Pucadyil, T. J.; Kalipatnapu, S.; Chattopadhyay, A. The serotonin$_{1A}$ receptor: a representative member of the serotonin receptor family. *Cell. Mol. Neurobiol.* **2005**, *25*, 553−580.
(43) Kalipatnapu, S.; Chattopadhyay, A. Membrane organization and function of the serotonin$_{1A}$ receptor. *Cell. Mol. Neurobiol.* **2007**, *27*, 1097−1116.
(44) Müller, C. P.; Carey, R. J.; Huston, J. P.; De Souza Silva, M. A. Serotonin and psychostimulant addiction: focus on 5-HT$_{1A}$-receptors. *Prog. Neurobiol.* **2007**, *81*, 133−178.
(45) Glikmann-Johnston, Y.; Saling, M. M.; Reutens, D. C.; Stout, J. C. Hippocampal 5-HT$_{1A}$ receptor and spatial learning and memory. *Front. Pharmacol.* **2015**, *6*, 289.
(46) Sarkar, P.; Kumar, G. A.; Pal, S.; Chattopadhyay, A. Biophysics of serotonin and the serotonin$_{1A}$ receptor: fluorescence and dynamics. In *Serotonin: The Mediator that Spans Evolution*; Pilowsky, P., Ed.; Elsevier: Amsterdam, 2018; pp 3−22.
(47) Albert, P. R.; Vahid-Ansari, F. The 5-HT$_{1A}$ receptor: Signaling to behavior. *Biochimie* **2019**, *161*, 34−45.
(48) Sarkar, P.; Mozumder, S.; Bej, A.; Mukherjee, S.; Sengupta, J.; Chattopadhyay, A. Structure, dynamics and lipid interactions of serotonin receptors: excitements and challenges. *Biophys. Rev.* **2021**, *13*, 101−122.
(49) Lacivita, E.; Leopoldo, M.; Berardi, F.; Perrone, R. 5-HT$_{1A}$ receptor, an old target for new therapeutic agents. *Curr. Top. Med. Chem.* **2008**, *8*, 1024−1034.
(50) Fiorino, F.; Severino, B.; Magli, E.; Ciano, A.; Caliendo, G.; Santagada, V.; Frecentese, F.; Perissutti, E. 5-HT$_{1A}$ receptor: an old target as a new attractive tool in drug discovery from central nervous system to cancer. *J. Med. Chem.* **2014**, *57*, 4407−4426.
(51) Edidin, M. Getting there is only half the fun. *Curr. Top. Membr.* **1996**, *43*, 1−13.
(52) Sarkar, P.; Chattopadhyay, A. Insights into cellular signaling from membrane dynamics. *Arch. Biochem. Biophys.* **2021**, *701*, 108794.
(53) Clausen, M. P.; Lagerholm, B. C. Visualization of plasma membrane compartmentalization by high-speed quantum dot tracking. *Nano Lett.* **2013**, *13*, 2332−2337.
(54) Kusumi, A.; Fujiwara, T. K.; Chadda, R.; Xie, M.; Tsunoyama, T. A.; Kalay, Z.; Kasai, R. S.; Suzuki, K. G. N. Dynamic organizing principles of the plasma membrane that regulate signal transduction: commemorating the fortieth anniversary of Singer and Nicolson's fluid-mosaic model. *Annu. Rev. Cell Dev. Biol.* **2012**, *28*, 215−250.
(55) Kusumi, A.; Nakada, C.; Ritchie, K.; Murase, K.; Suzuki, K.; Murakoshi, H.; Kasai, R. S.; Kondo, J.; Fujiwara, T. Paradigm shift of the plasma membrane concept from the two-dimensional continuum fluid to the partitioned fluid: high-speed single-molecule tracking of membrane molecules. *Annu. Rev. Biophys. Biomol. Struct.* **2005**, *34*, 351−378.
(56) Fujiwara, T.; Ritchie, K.; Murakoshi, H.; Jacobson, K.; Kusumi, A. Phospholipids undergo hop diffusion in compartmentalized cell membrane. *J. Cell Biol.* **2002**, *157*, 1071−1081.
(57) Ganguly, S.; Chattopadhyay, A. Cholesterol depletion mimics the effect of cytoskeletal destabilization on membrane dynamics of the serotonin$_{1A}$ receptor: A *z*FCS study. *Biophys. J.* **2010**, *99*, 1397−1407.
(58) Shrivastava, S.; Sarkar, P.; Preira, P.; Salomé, L.; Chattopadhyay, A. Role of actin cytoskeleton in dynamics and function of the serotonin$_{1A}$ receptor. *Biophys. J.* **2020**, *118*, 944−956.
(59) Day, C. A.; Kenworthy, A. K. Tracking microdomain dynamics in cell membranes. *Biochim. Biophys. Acta* **2009**, *1788*, 245−253.
(60) Chen, Y.; Lagerholm, B. C.; Yang, B.; Jacobson, K. Methods to measure the lateral diffusion of membrane lipids and proteins. *Methods* **2006**, *39*, 147−153.
(61) Jacobson, K.; Liu, P.; Lagerholm, B. C. The lateral organization and mobility of plasma membrane components. *Cell* **2019**, *177*, 806−819.
(62) Sarkar, P.; Chattopadhyay, A. Exploring membrane organization at varying spatiotemporal resolutions utilizing fluorescence-based approaches: implications in membrane biology. *Phys. Chem. Chem. Phys.* **2019**, *21*, 11554−11563.
(63) Lagerholm, B. C.; Weinreb, G. E.; Jacobson, K.; Thompson, N. L. Detecting microdomains in intact cell membranes. *Annu. Rev. Phys. Chem.* **2005**, *56*, 309−336.
(64) Kasai, R. S.; Kusumi, A. Single-molecule imaging revealed dynamic GPCR dimerization. *Curr. Opin. Cell Biol.* **2014**, *27*, 78−86.
(65) Yu, J. Single-molecule studies in live cells. *Annu. Rev. Phys. Chem.* **2016**, *67*, 565−585.
(66) Marguet, D.; Salomé, L. Lateral diffusion in heterogeneous cell membranes. In *Physics of Biological Membranes*; Bassereau, P., Sens, P., Ed.; Springer Nature: 2018; pp 169−189.
(67) Destainville, N.; Dumas, F.; Salomé, L. What do diffusion measurements tell us about membrane compartmentalisation? Emergence of the role of interprotein interactions. *J. Chem. Biol.* **2008**, *1*, 37−48.
(68) Shen, H.; Tauzin, L. J.; Baiyasi, R.; Wang, W.; Moringo, N.; Shuang, B.; Landes, C. F. Single particle tracking: from theory to biophysical applications. *Chem. Rev.* **2017**, *117*, 7331−7376.
(69) Haanappel, E.; Salomé, L. G-protein-coupled receptors: membrane diffusion and organization matter. In *Springer Series in Biophysics. Membrane Organization and Dynamics*; Chattopadhyay, A., Ed.; Springer International: 2017; Vol. *20*, pp 243−258.
(70) Wieser, S.; Schütz, G. J. Tracking single molecules in the live cell plasma membrane-do's and don't's. *Methods* **2008**, *46*, 131−140.
(71) Daumas, F.; Destainville, N.; Millot, C.; Lopez, A.; Dean, D.; Salomé, L. Confined diffusion without fences of a G-protein-coupled receptor as revealed by single particle tracking. *Biophys. J.* **2003**, *84*, 356−366.
(72) Veya, L.; Piguet, J.; Vogel, H. Single molecule imaging deciphers the relation between mobility and signaling of a prototypical G protein-coupled receptor in living cells. *J. Biol. Chem.* **2015**, *290*, 27723−27735.
(73) Kumar, G. A.; Sarkar, P.; Jafurulla, M.; Singh, S. P.; Srinivas, G.; Pande, G.; Chattopadhyay, A. 2019. Exploring endocytosis and intracellular trafficking of the human serotonin$_{1A}$ receptor. *Biochemistry* **2019**, *58*, 2628−2641.
(74) Shrivastava, S.; Pucadyil, T. J.; Paila, Y. D.; Ganguly, S.; Chattopadhyay, A. Chronic cholesterol depletion using statin impairs the function and dynamics of human serotonin$_{1A}$ receptors. *Biochemistry* **2010**, *49*, 5426−5435.
(75) Pucadyil, T. J.; Chattopadhyay, A. Cholesterol depletion induces dynamic confinement of the G-protein coupled serotonin$_{1A}$ receptor in the plasma membrane of living cells. *Biochim. Biophys. Acta* **2007**, *1768*, 655−668.
(76) Amundson, D. M.; Zhou, M. (1999) Fluorometric method for the enzymatic determination of cholesterol. *J. Biochem. Biophys. Methods* **1999**, *38*, 43−52.
(77) Smith, P. K.; Krohn, R. I.; Hermanson, G. T.; Mallia, A. K.; Gartner, F. H.; Provenzano, M. D.; Fujimoto, E. K.; Goeke, N. M.; Olson, B. J.; Klenk, D. C. Measurement of protein using bicinchoninic acid. *Anal. Biochem.* **1985**, *150*, 76−85.
(78) Sergé, A.; Bertaux, N.; Rigneault, H.; Marguet, D. Dynamic multiple-target tracing to probe spatiotemporal cartography of cell membranes. *Nat. Methods* **2008**, *5*, 687−694.

https://doi.org/10.1021/acs.jpcb.2c03941
J. Phys. Chem. B 2022, 126, 6682−6690

(79) Meilhac, N.; Le Guyader, L.; Salome, L.; Destainville, N. Detection of confinement and jumps in single-molecule membrane trajectories. *Phys. Rev. E* **2006**, *73*, 011915.
(80) Roy, S.; Kumar, G. A.; Jafurulla, M.; Mandal, C.; Chattopadhyay, A. Integrity of the actin cytoskeleton of host macrophages is essential for *Leishmania donovani* infection. *Biochim. Biophys. Acta* **2014**, *1838*, 2011−2018.
(81) Ganguly, S.; Saxena, R.; Chattopadhyay, A. Reorganization of the actin cytoskeleton upon G-protein coupled receptor signaling. *Biochim. Biophys. Acta* **2011**, *1808*, 1921−1929.
(82) Kumar, G. A.; Sarkar, P.; Stepniewski, T. M.; Jafurulla, M.; Singh, S. P.; Selent, J.; Chattopadhyay, A. A molecular sensor for cholesterol in the human serotonin$_{1A}$ receptor. *Sci. Adv.* **2021**, *7*, eabh2922.
(83) Cuatrecasas, P. Membrane receptors. *Annu. Rev. Biochem.* **1974**, *43*, 169−214.
(84) Kahn, C. R. Membrane receptors for hormones and neurotransmitters. *J. Cell Biol.* **1976**, *70*, 261−286.
(85) Peters, R. Lateral mobility of proteins and lipids in the red cell membrane and the activation of adenylate cyclase by *β*-adrenergic receptors. *FEBS Lett.* **1988**, *234*, 1−7.
(86) Sarkar, P.; Chakraborty, H.; Chattopadhyay, A. Differential membrane dipolar orientation induced by acute and chronic cholesterol depletion. *Sci. Rep.* **2017**, *7*, 4484.
(87) Zidovetzki, R.; Levitan, I. Use of cyclodextrins to manipulate plasma membrane cholesterol content: Evidence, misconceptions and control strategies. *Biochim. Biophys. Acta* **2007**, *1768*, 1311−1324.
(88) Mahammad, S.; Parmryd, I. Cholesterol depletion using methyl-*β*-cyclodextrin. *Methods Mol. Biol.* **2015**, *1232*, 91−102.
(89) Endo, A. A gift from nature: The birth of the statins. *Nat. Med.* **2008**, *14*, 1050−1052.
(90) Mascalchi, P.; Haanappel, E.; Carayon, K.; Mazères, S.; Salomé, L. Probing the influence of the particle in single particle tracking measurements of lipid diffusion. *Soft Matter* **2012**, *8*, 4462−4470.
(91) Baier, C. J.; Gallegos, C. E.; Levi, V.; Barrantes, F. J. Cholesterol modulation of nicotinic acetylcholine receptor surface mobility. *Eur. Biophys. J.* **2010**, *39*, 213−227.
(92) Vrljic, M.; Nishimura, S. Y.; Moerner, W. E.; McConnell, H. M. Cholesterol depletion suppresses the translational diffusion of class II major histocompatibility complex proteins in the plasma membrane. *Biophys. J.* **2005**, *88*, 334−347.
(93) Kenworthy, A. K.; Nichols, B. J.; Remmert, C. L.; Hendrix, G. M.; Kumar, M.; Zimmerberg, J.; Lippincott-Schwartz, J. Dynamics of putative raft-associated proteins at the cell surface. *J. Cell. Biol.* **2004**, *165*, 735−746.
(94) Nishimura, S. Y.; Vrljic, M.; Klein, L. O.; McConnell, H. M.; Moerner, W. E. Cholesterol depletion induces solid-like regions in the plasma membrane. *Biophys. J.* **2006**, *90*, 927−938.
(95) Faulstich, H.; Zobeley, S.; Rinnerthaler, G.; Small, J. V. Fluorescent phallotoxins as probes for filamentous actin. *J. Muscle Res. Cell Motil.* **1988**, *9*, 370−383.

https://doi.org/10.1021/acs.jpcb.2c03941
J. Phys. Chem. B 2022, 126, 6682−6690